Formulation and characterization of folate conjugated PEG spacer based nanoparticle for the effective targeting against breast cancer cell line

Anjalee Kushwaha,[1]* Dr. Arun Patel,[2] Dr. Naveen Shivavedi[3]
Dr. Shailendra Patel[4]

*[1*2,3,4]Shri Ram Group of Institutions, Department of Pharmacy,Jabalpur-482002 M.P.,India.*

***Corresponding Author:**Anjalee Kushwaha.
***Gmail:**anjaleekushwaha469@gmail.com

Abstract

Now days, breast cancer is the most frequently diagnosed life-threatening cancer in women and the leading cause of cancer death among women. The objective of present study was to design various PEG based nanosystems in which folic acid is attached directly or indirectly via different types of PEGs (Mw: 1000, 4000) as spacers and resolve possible shortcomings associated with cancer chemotherapy. An anti-cancer bioactive was encapsulated in above types of SLN nanoconjugates and their in vitro as well as ex vivo anticancer targeting potential compared. Above studies (FT-IR, 1HNMR and TEM studies) concluded that the folate are attached directly and indirectly via PEGs as spacer to the SLNs. There after these developed nanoconjugates formulations were optimized for the drug loading, drug entrapment, cumulative drug release and tumor targeting potential by ex vivo cell line study. The present work is expected to throw new light on the role of spacer chain length in targeting potential of folate anchored SLN. The drug entrapment, surface morphology, particle size, PDI, and in vitro drug release. In order to authenticate the provided PTX samples as well as to determine vital physicochemical parameters that can aid during synthesis/formulation development, preformulation studies were carried out. The drug entrapment efficiency of plain SLN was 79.30.5 percent, which was greater than the drug entrapment efficiency of connected SLN, which was 71.7 percent. In each steps, the outcomes of the studies were compared with standard pharmacopoeial guidelines.

Introduction

Cancer is a multifaceted disease that represents one of the leading causes of mortality in developed countries. Due to the societal and economical implications of this pathology, tremendous efforts have been made over the past decades to improve the available therapeutic options. Although a large number of potent chemotherapeutic anticancer agents have been identified and successfully used in clinical practice, considerable research activity is devoted to discover more potent treatments, while minimizing their toxic side effects.

Indeed, most anticancer agents display a narrow therapeutic window due to their lack of selectivity against cancer cells. Besides, the ability of the anticancer compounds to actually reach their target is often impaired by a number of physiological barriers (i.e., tumour interstitial pressure, diffusion through the tumour endothelium and/or extracellular matrix and so on) as well as by metabolisation/degradation phenomena such as conversion into inactive metabolites.[1]

Tumors are characterized by poorly differentiated, highly chaotic arrangement of vessels which have unsealed endothelial cell– cell junctions and discontinuous basement membrane. Due to their irregular organization, tumor microvessel walls are leaky and exhibit heterogeneous hyperpermeability compared to normal tissue (Jain & Stylianopoulos, 2010). Unlike normal tissues, tumors have functionally defective lymphatic vessels because cancer cells compress lymphatic vessels causing their collaps. Also, the decreased lymphatic drainage associated with tumors results in retention of permeated macromolecules in tumors. The fluid that leaves the bloodstream inside the tumor can only escape from the tumor either by feeding back into post capillary venules or by passage through the tumor interstitium.

Tumor cell targeting is a promising strategy for enhancing the therapeutic potential of chemotherapy agents. PEG coated (sterically stabilized) carrier show enhanced accumulation on the surface of tumors, but steric hindrance by PEGylation reduces the association of the carrier-bound ligand with its receptor. FR targeting depends upon the concentration and PEG spacer length of folate-PEG-carrier conjugates. PEG conjugation or linking with the SLNs system is called PEGylation, which improves water solubility and non-statistical attachment of drug molecules. The main purposes of PEGylation of SLNs are to alter biodistribution and pharmacokinetics of SLNs. PEGylation of SLNs can generally overcome reticuloendothelial system (RES) uptake, drug leakage, immunogenicity, hemolytic toxicity, cytotoxicity, hydrophobicity. Hemolytic and different cell line studies have shown reduced toxicity of PEGylated SLNs than cationic SLNs. PEGylation causes increased solubilization of hydrophobic drugs in SLNs framework as well as in PEG layers. PEGylated SLNs show longer blood retention and lower accumulation in other normal organs than the non-PEGylated SLNs.

Materials and methods

Preformulation study

Preformulation studies are needed to ensure the development of a stable as well as therapeutically effective and safe dosage form and preformulation studies of the drug PTX include identification, physical appearance, melting point, solubility, standard curve and partition coefficient.

Identification of drug

Physical Appearance

The drug PTX gifted from SUN Pharmaceutical Industries Ltd- Gujarat (India). The supplied powder of PTX was White to off-white crystalline powder

Melting Point

Melting point of PTX was determined by melting point apparatus and found to be 216°-217°C.

The sample was qualitatively tested for its solubility in various solvents. It was determined by taking 2 mg of drug sample in 5 ml of solvent as Distilled water, PBS 7.4,ethanol, Diethyl ether, chloroform, Dimethyl sulfoxide (DMSO) etc., in test tubes using a vortex shaker (Yorco, New Delhi). The results obtained by solubility testing are given in (Table 4.1).

Determination of partition coefficient

The partition behavior of drug was examined in n-Octanol: Water, and n-Octanol: PBS (pH 7.4) systems.

$$\text{The partition cofficient} = \frac{\text{Amount of drug in organic layer}}{\text{Amount of drug in aqueous layer}}$$

Determination of λmax

The PTX (10.0 mg) was accurately weighed and dissolved in approximately 5 ml of methanol. Volume was made up to 100 ml with 30:70 methanols: PBS (pH 7.4) to give a stock solution of 100 mg/ml. Then make 2 μg/ml aliquate and scanned between 200-400 nm absorption maxima on a UV/Visible spectrophotometer (Shimadzu 1800, Japan). The λmax was found to be 237.0 nm.

Infrared spectroscopy of ptx

It was done by making pellets of the drug in KBr. IR spectra was taken in Dr.Hari singh gour viswavidyalaya,sagar. The observed peaks were compared with those (USP NF, 2007) reported for functional groups (Table 4.3, Figure 4.2 and 4.3).

Calibration curve of ptx

As mentioned in I.P. 2007. 2.38 g disodium hydrogen orthophosphate, 0.19 g potassium dihydrogen orthophosphate and 8.0 g sodium chloride were mixed in about 100 ml of distilled water and the volume was made up 1000 ml with distilled water, the pH of solution was adjusted to 7.4 immediately before use with 0.1N hydrochloric acid or 0.1 N NaOH as required.

Drug compatibility studies with selected lipids

Drug compatibility with soya phosphatidyl choline (SPC) and tristearin was studied. Solution of PTX (20μg/ml) was prepared in PBS (pH 7.4) using methanol as cosolvent.

RESULTS AND DISCUSSION

PTX was gifted from SUN Pharma Industries Ltd and identified as per tests prescribed in Pharmacopoeia of India (2007). An infrared spectrum of provided drug was found to be concordant with the reference infrared spectrum of the PTX given in Martindale. Solubility study in different solvents at room temperature revealed that it is soluble in Ethanol, Chloroform, DMSO, and insoluble in distilled water etc. Partition coefficient value of PTX also revealed & it is Lipophilic nature {$P_{O/W}$ = 3.50 for n-Octanol/ water, 3.59 for n-Octanol/PBS (pH 7.4) . An acidic solution of PTX was scanned in the U.V. range of 200-400 nm using Shimadzu 1800 UV Visible spectrophotometer as prescribed in I.P. 2007.

The Spectrophotometric method of analysis of PTX at λ_{max} 237.0 nm was found to be reproducible and highly sensitive. The standard curves of PTX were prepared in phosphate buffer solution (pH 7.4) at λ_{max} 237.0 nm,. The data were regressed to obtain the straight line.

The correlation coefficient 0.997 was observed in all the cases, which indicated that, the drug follows Beer-Lambert's law in the concentration range of 2-20 µg/ml. In the present study, polymers were selected on the basis of their solubility's and non-interference in the estimation of drug. The absorbance data of both drug and different additives were noted. The absorbance data had shown no appreciable change in the absorbance of drug solution at 237.0 nm indicating no interference of polymers in the estimation of PTX. PTX analysed by HPLC at λ_{max} 237.0 nm .A Mobile phase consisting of Methanol and 0.02 M potassium dihydrogen phosphate in water (pH 2.5 adjusted with o-phosphoric acid) in the ratio of 80:20 v/v was used. The flow rate was 1 ml/min. The retention time was found 3.087 min.

Table 1: Solubility of PTX in different solvents

S. No.	Solvent	Solubility
1.	Distilled Water	-
2.	PBS (pH 7.4)	-
3.	Ethanol	++++
4.	Chloroform	++++
5.	Diethyl ether	++
6.	Dimethyl sulfoxide (DMSO)	++++

++++ Freely soluble 1-10 parts,
+++ Sparingly soluble 30-100 parts,
++ Soluble 30-100 parts,
+ Slightly soluble 100-1000 parts,
– Practically insoluble >10000 parts

Table 2: Partition coefficient values of PTX

S. No.	Solvent system	Partition Coefficient
1.	n-Octanol/Distilled water	3.50
2.	n-Octanol/PBS (pH 7.4)	3.59

Table 3: Important band frequencies in IR spectrum of PTX

S. No.	Wave No.(cm^{-1})	Description
1.	3509.8	OH stretching
2.	3245.7	NH stretching
3.	3019.0	=CH Stretching (Aromatic)
4.	1737.6	C=O Stretching
5.	1645.33	C=O Amide

Table 4: Standard Curve of PTX in Phosphate Buffer Solution (pH 7.4) at λ_{max} 237.0 nm

S.No.	Drug Conc. (µg/ml)	Absorbance	Regressed Absorbance	Statistical Parameters
1.	2	0.0990	0.1116	
2.	4	0.1594	0.1706	
3.	6	0.1982	0.2269	
4.	8	0.2659	0.2886	y = 0.033x + 0.011
5.	10	0.3419	0.3476	R^2 = 0.997
6.	12	0.4187	0.4066	
7.	14	0.4814	0.4656	
8.	16	0.5486	0.5246	
9.	18	0.6137	0.5836	
10.	20	0.6845	0.6625	

Table 5: Compatibility testing of drug with ingredient lipids

S. No.	Composition	Absorption maxima λmax (nm)	Absorbance
1.	PTX	237	0.5146
2.	PTX + SPC	237	0.5069
3.	PTX + Tristearin	237	0.4889

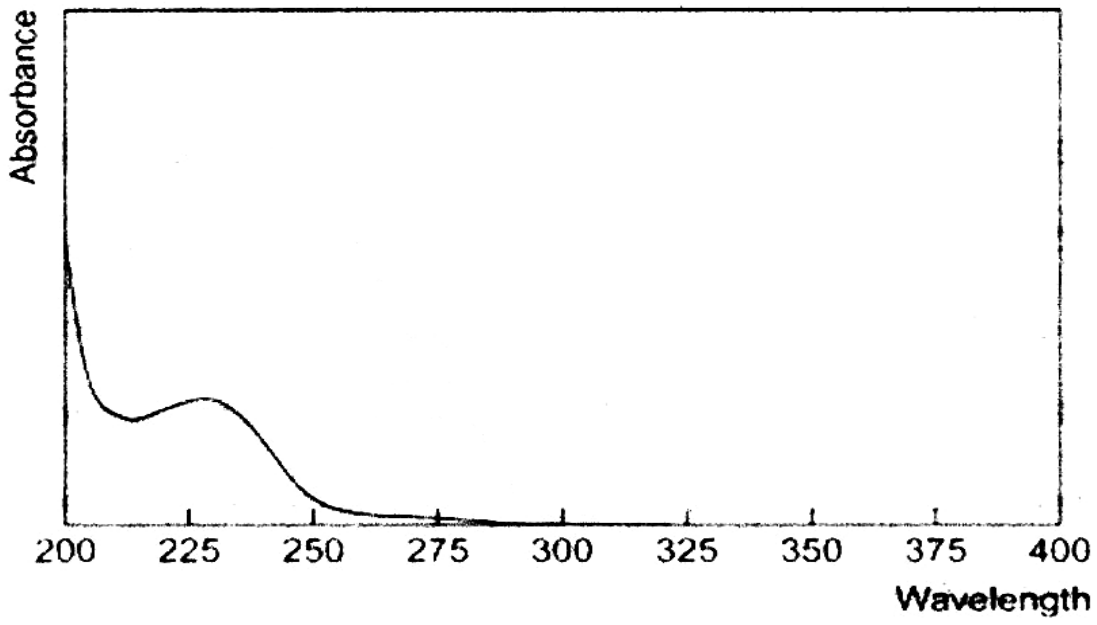

(a)

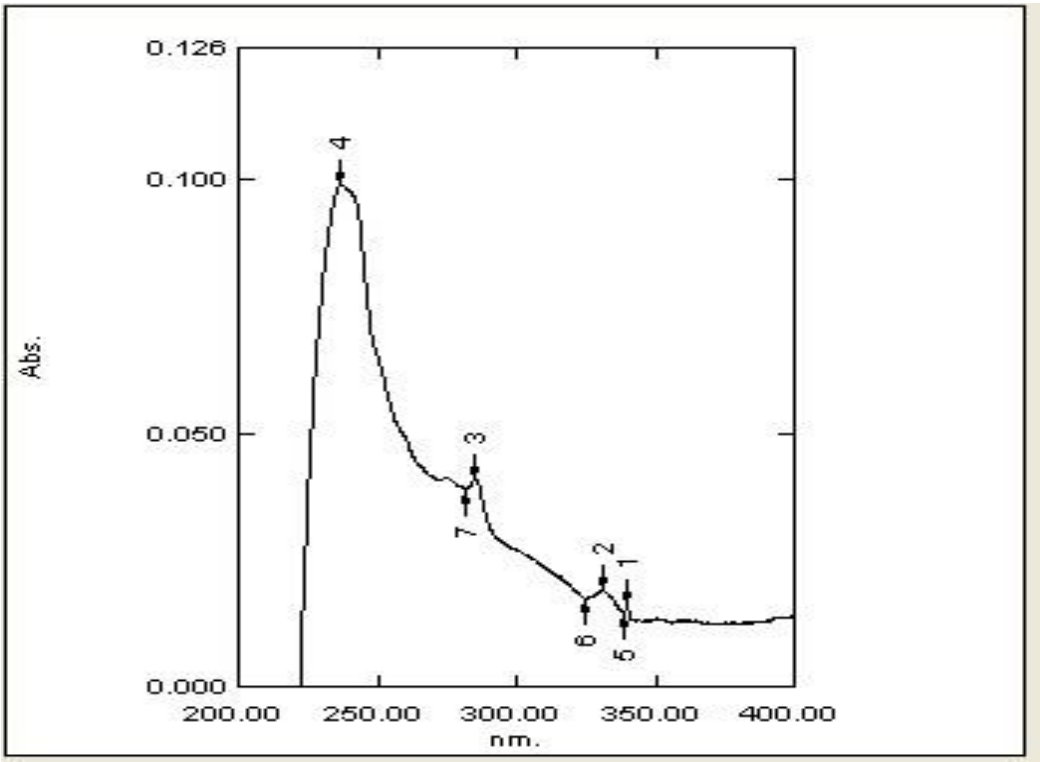

(b)

Figure 1: Absorption maxima of PTX (a) Reference (b) Sample

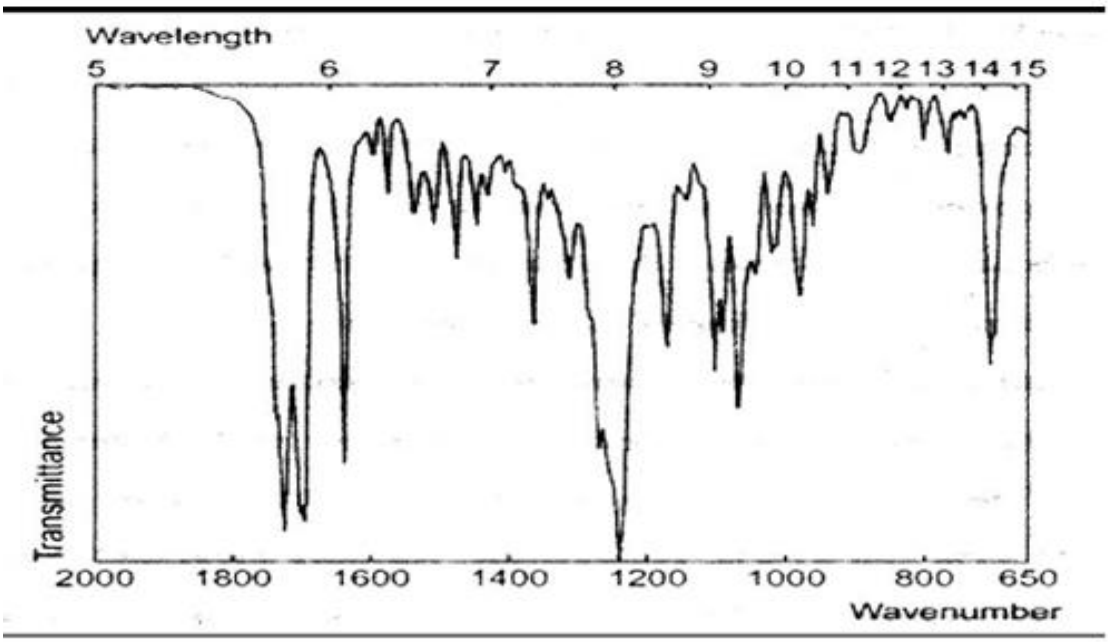

Figure 2: Standard IR spectra of PTX

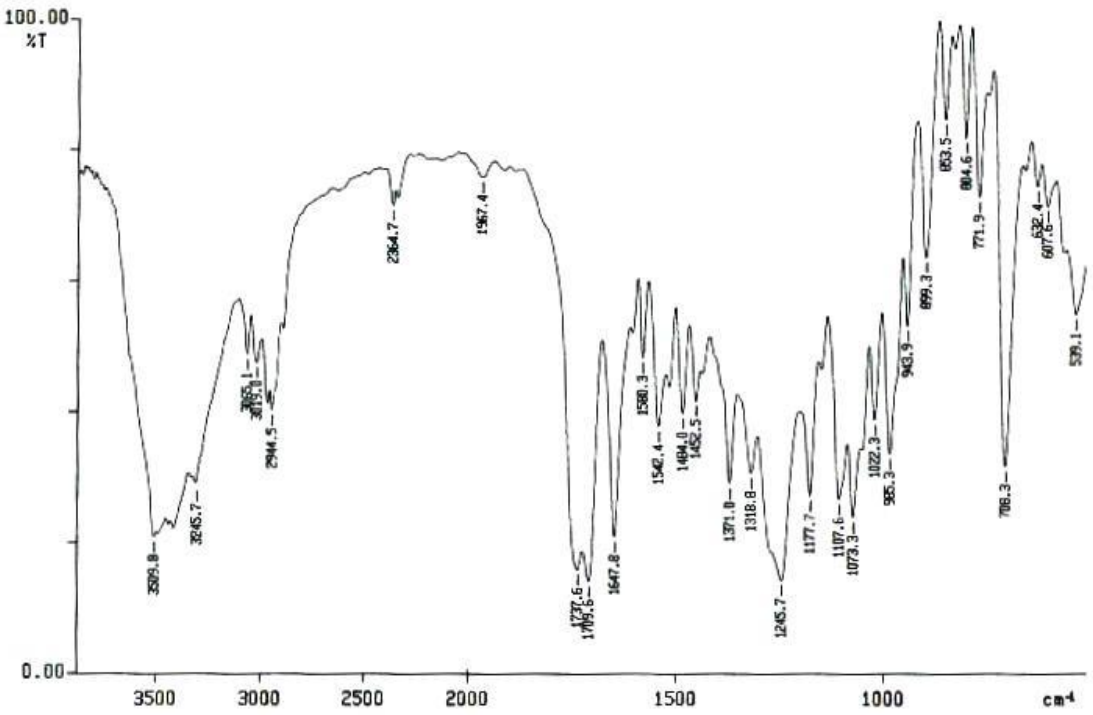

Figure 3: IR spectra of PTX (Sample)

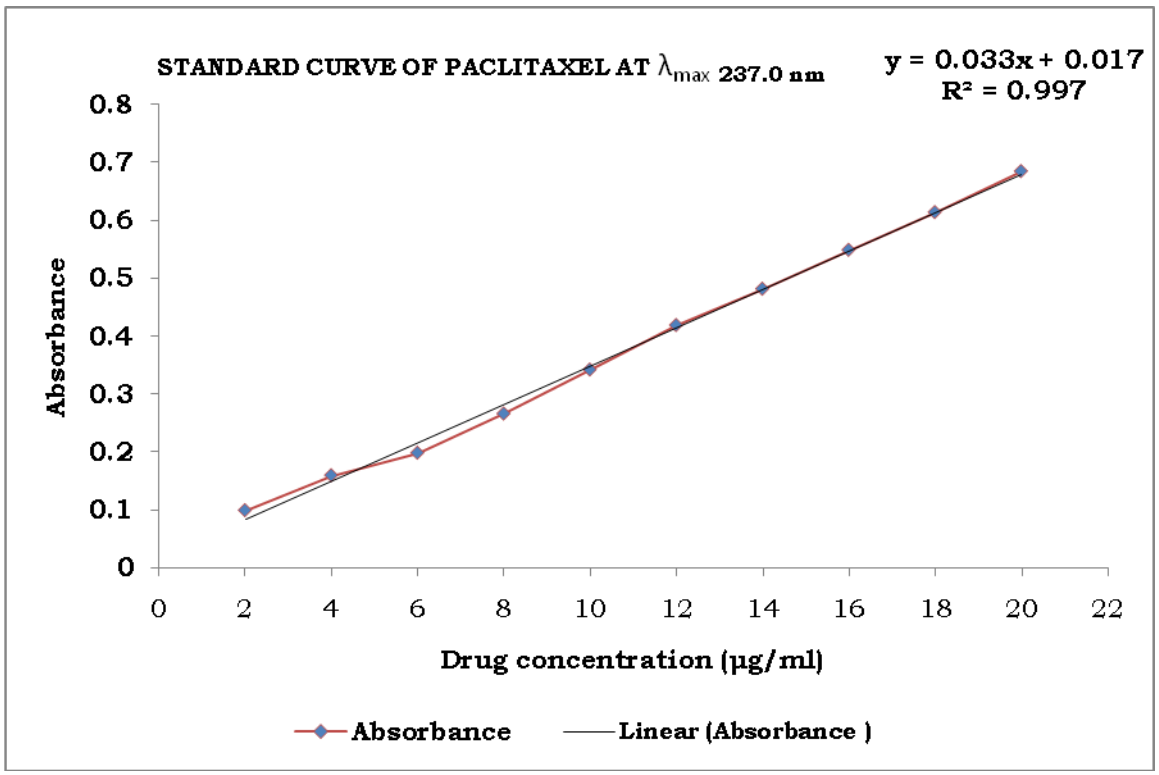

Figure 4: UV absorption maxima of PTX in Phosphate Buffer Solution (pH 7.4) at λ_{max} 237.0 nm

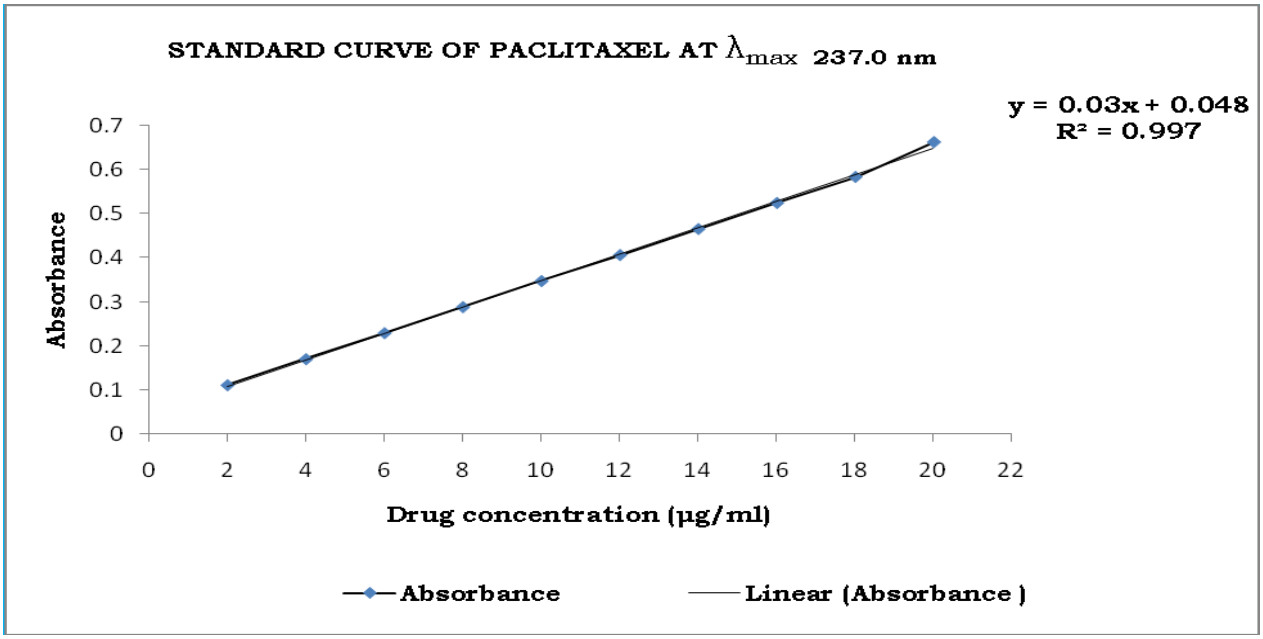

Figure 5: Linearly regressed standard curve of PTX in phosphate buffer solution (pH 7.4) at λ_{max} 237.0 nm

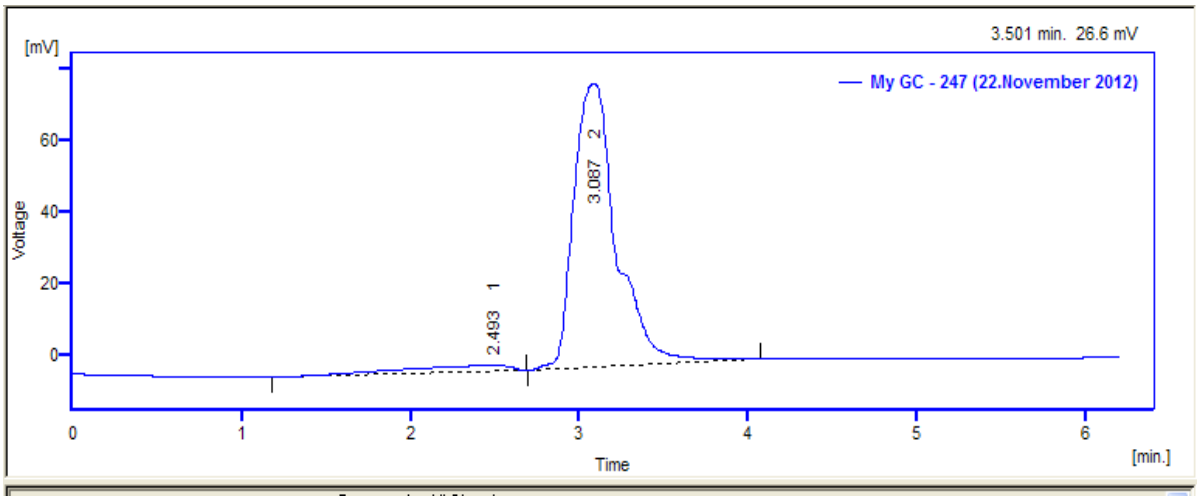

Figure 6: HPLC analysis of PTX

Sun Pharmaceutical Industries Ltd, Gujarat, sent paclitaxel as a gift (India). Himedia provided the Soya Phosphatidyl Choline (SPC). Unless otherwise noted, all additional reagents and solvents were analytical grade and bought from local vendors. Throughout the investigation, deionized water was utilised.

5.2 PREPARATION OF SOLID LIPID NANOPARTICLE

The solid lipid nanoparticles were prepared by solvent injection method as reported by Hu *et al*., 2008[82]. Tristearin, soya lecithin, stearylamine and drug (10mg) were taken into different ratio and were dissolved in minimum quantity of absolute alcohol and heated about 70^0C in a beaker. Tween 80 (0.5 % v/v) was dissolved in distilled water and heated at about 70^0C. Then the organic phase i.e. alcoholic solution containing lipid mixture and drug was added to preheated aqueous solution at the same temperature (about 70 ^{0}C) at constant stirring.

Determination of particle size

Using a Zetasizer DTS ver. 4.10, photon correlation spectroscopy was being used to measure the average particle size and size distribution of solid lipid nanoparticles (Malvern Instrument, UK).

Measurement of the surface charge

The surface charge of solid lipid nanoparticles was evaluated by measuring the zeta potential of the lipid nanoparticles, which was estimated from their electrophoretic mobility according to Helmholtz-Smoluchowsky.

Morphology of Particles (TEM)

The particle morphology was seen using a transmission electron microscope. The sample (10L) was placed on the grids and allowed to stand at room temperature for 90 seconds. Excess fluid was removed by gently brushing the edge of the filter paper with a finger.

Effectiveness of Entrapment

The drug entrapment of the PTX in SLNs was estimated by dispersing the known molar concentration of paclitaxel loaded SLNs in a cellulose dialysis bag (MWCO 1000 Da, Sigma, Germany). To remove any unentrapped drug from the formulation, it was dialyzed against PBS (pH 7.4) in a cellulose dialysis bag for 10 minutes under sink conditions utilising magnetic stirring (50 rpm; Remi, Mumbai, India).

Drug Release in Vitro

Presoaked dialysis bag (MWCO 12– 14 kDa, Hi Media, India) was used to release PTX loaded SLNs and Folate linked SLNs in PBS (pH 7.4).

Table 1: Particle Size, PDI, % Drug Entrapment

Formulation Code	Size	Polydispersity Index	% Drug Entrapped
Plain SLNs	201.1 ± 3.7	0.224	31.09±0.71
Folate coupled SLNs SLNFA	249.4 ± 2.6	0.238	48.01±0.92
SLNP1FA	293.4± 3.4	0.325	52.98±0.33
SLNP4FA	315.0± 3.4	0.395	58.22±0.51

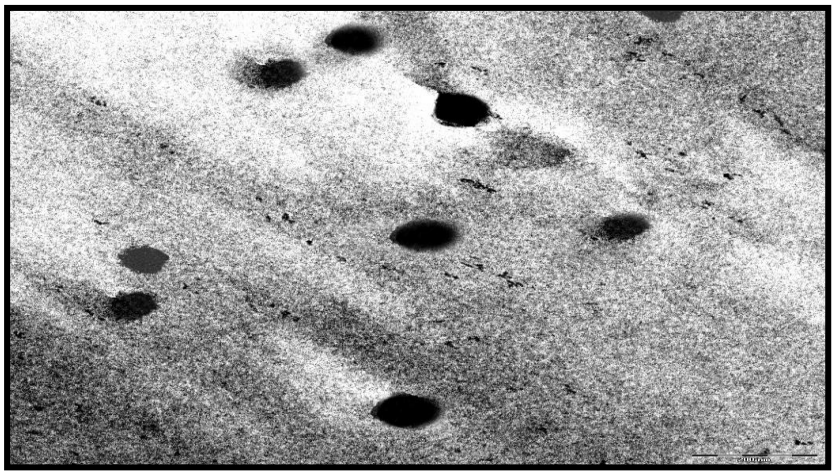

Figure 5.1: TEM image of plain SLNs

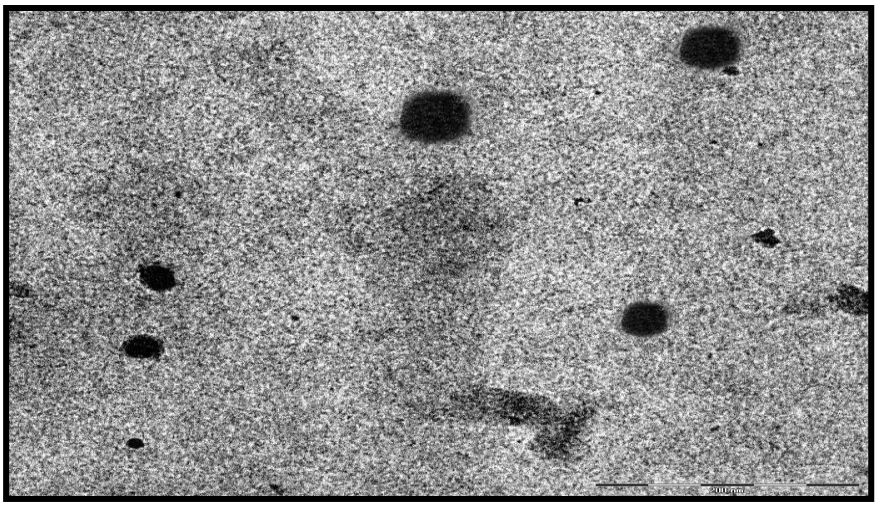

Figure 5.2: TEM image of coupled SLNs

RESULTS AND DISCUSSION

Simple SLNs were created using the solvent injection method, which involves quick solvent diffusion across the solvent-lipid phase into the aqueous phase. Tentaarin, PC, stearylamine, and medicine were dissolved in ethanol and held at a high temperature of 70 degrees Celsius with continual stirring. This solution was injected into a Tween 80 aqueous solution, which was sonicated using a probe sonicator at the same temperature as previously. The drug's in vitro release was studied after the formulation was linked with the ligand and characterised (Table 5.2). The form and surface morphology of the particles were studied using SEM and TEM. Particle size, polydispersity index, and zeta potential were investigated using the Laser Light Scattering technique (Malvern Instrument).

The PDI of plain SLNs was 0.224, with an average particle size of 201.13.7 nm, as shown in Table 5.1. Drug entrapment was measured using dialysis with a dialysis membrane, and it was determined to be 79.30.5 percent. The drug entrapment, surface morphology, particle size, PDI, and in vitro drug release. Paclitaxel-loaded plain SLNs had a particle size of 201.13.7 nm, which was smaller than paclitaxel-loaded Folate linked SLNs, which had a particle size of 249.42.6 nm. This might be due to the Folate coating on the surface of SLNs forming an additional layer on top of the SLN surface. Plain formulations exhibited a lower PDI (0.224) than connected formulations (0.238), which might be due to the SLN's surface being disrupted by the Folate coupling. The drug entrapment efficiency of plain SLN was 79.30.5 percent, which was greater than the drug entrapment efficiency of connected SLN, which was 71.70.5 percent. This might be because the medication escaped from the SLN during the incubation period (Table 5.1).

FT-IR Spectroscopy

The FT-IR spectroscopy methodology was used to characterise the synthesised nanoconjugates (SLNFA, SLNP1FA, and SLNP4FA) utilising Nujol's mull method was performed at Dr. H. S. Gour University Sagar (M.P.), by Elmer 783 Spectrophotometer.

Table 6.2: Important peaks of FT-IR spectrum and data analysis of SLNFA

Wave number (cm^{-1})	Interpretation
789.83	Aromatic C-H bend
1128.08	Ester unconjugated C=O stretching
3445.95	N-H stretching of primary amine and O-H stretching
1128.08	Ester unconjugated C=O stretching
2252.92	Alkynyl C-H and C=C stretching
1673.75	Aromatic C=C bending and stretching due to attachment of FA
1416.11	CH-NH-C(=O) amides bending
1261.26	Esters unconj. C=O and C-O stretching
819.83, 789.83	Aromatic C-H bending

Table 6.3: Important peaks of FT-IR spectrum and data analysis of SLNP1FA

Wave number (cm^{-1})	Interpretation
3435.86	N-H stretch of primary amine
2938.77, 2889.91	Carboxylic acid C=O and O-H stretch
1462.46, 1415.88	CH-NH-C(=O) amides bending
1228.75, 1192.07	Esters C-O stretching
1114.71	C-O stretch ether linkage strong
950.97, 819.41	Aromatic C-H bending

Table 6.4: Important peaks of FT-IR spectrum and data analysis of SLNP4FA

Wave number (cm^{-1})	Interpretation
3434.11	N-H stretch of primary amine
2923.72, 2871.61	Carboxylic acid C=O and O-H stretch
1643.13, 1735.88	
1458.03	CH-NH-C(=O) amides bending
1298.69, 1250.31	Esters C-O stretching
1107.21	C-O stretch ether linkage strong
950.80, 845.69	Aromatic C-H bending

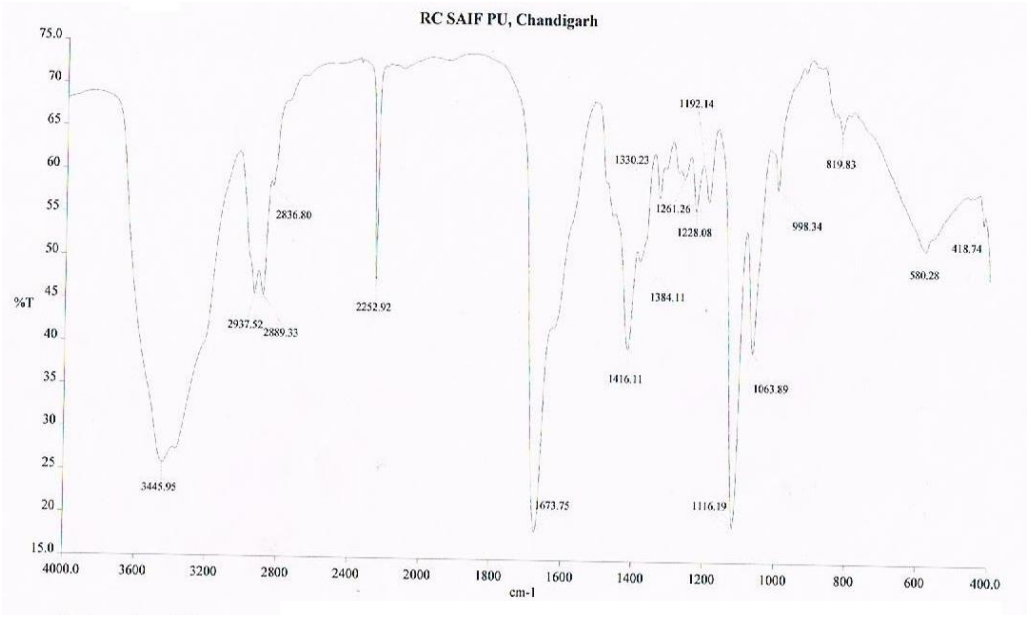

Figure 1: FT-IR spectrum of SLNFA

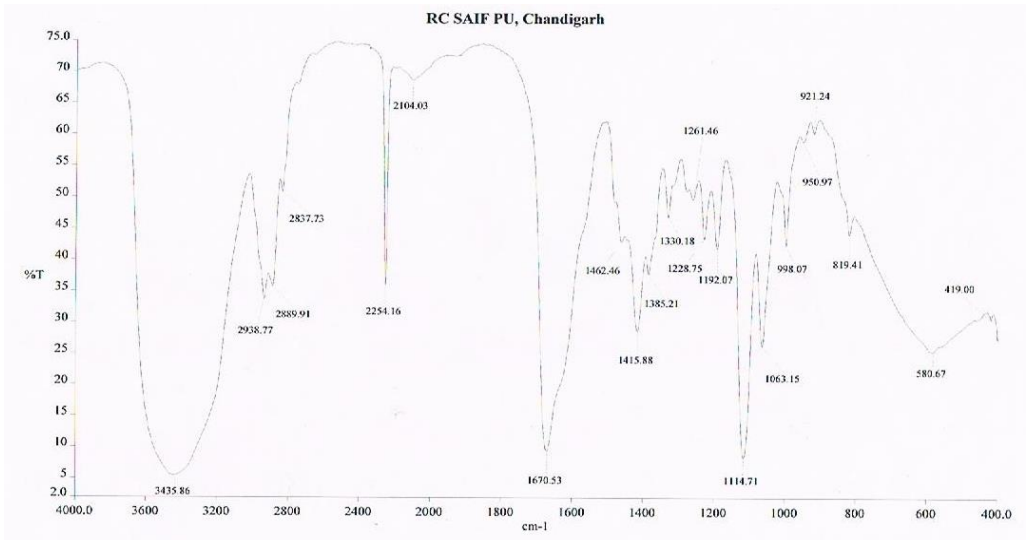

Figure 2: FT-IR spectrum of SLNP1FA

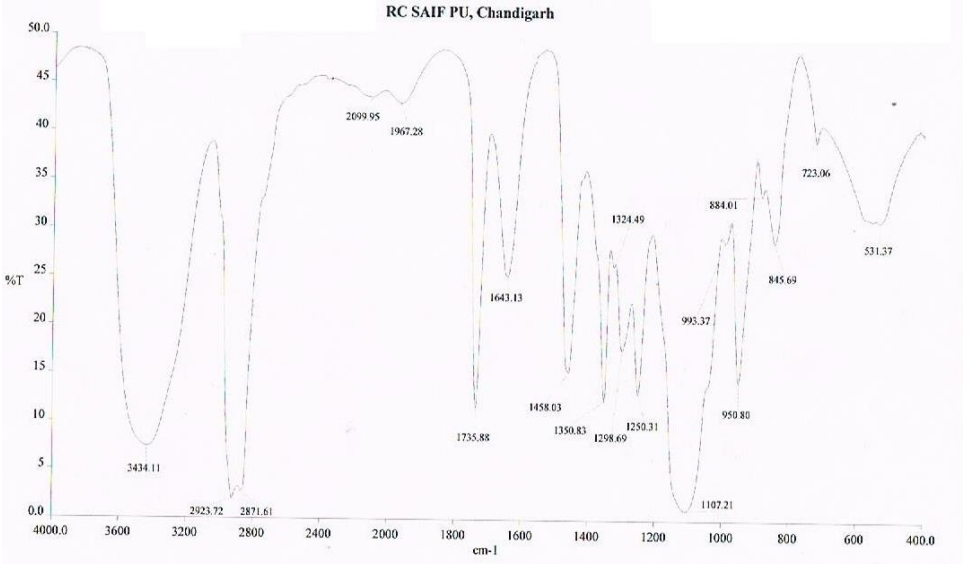

Figure 3: FT-IR spectrum of SLNP4FA

CONCLUSION

Above studies (FT-IR, ^{1}HNMR and TEM studies) concluded that the folate are attached directly and indirectly via PEGs as spacer to the SLNs. There after these developed nanoconjugates formulations were optimized for the drug loading, drug entrapment, cumulative drug release and tumor targeting potential by *ex vivo* cell line study.

The objective of present study was to design various SLNs based folate anchored nanosystems in which folic acid is attached directly or indirectly via different types of PEGs (Mw: 1000, 4000) as spacers and resolve possible shortcomings associated with cancer chemotherapy. An anti-cancer bioactive was encapsulated in above types of SLN nanoconjugates and their in vitro as well as ex vivo anticancer targeting potential compared. The present work is expected to throw new light on the role of spacer chain length in targeting potential of folate anchored SLN. In order to authenticate the provided PTX samples as well as to determine vital physicochemical parameters that can aid during synthesis/formulation development, preformulation studies were carried out. In each steps, the outcomes of the studies were compared with standard pharmacopoeial guidelines.

References

1. Bildstein L, Dubernet C, Couvreur P (2011) Prodrug-based intracellular delivery of anticancer agents. *Adv Drug Deliv Rev* 63, 3-23.
2. Boltri L., Canal T., Esposito P.A., Carli F.,(1993), Lipid nanoparticles: Evaluation of some critical formulation parameters, *Proc Intern Symp Control Rel Bioact Mater*, 20:346-47.
3. Cavalli R., Caputo O., Gasco M.R., (2000), Preparation and characterization of solid lipid nanoparticle containing Paclitaxel, *Eur J Pharma Sc,*10: 305-09.
4. Chattopadhyay P., Shekunov B.Y., Yim D., Cipolla D., Boyd B., Farr S., (2007), Production of solid lipid nanoparticle suspensions using supercritical fluid extraction of emulsions (SFEE) for pulmonary delivery using the AERx system, Adv Drug Deliv Rev., 59:444-53.
5. Chen H., Chang X., Du D., Liu W., Liu J., Weng T., (2006), Podophyllotoxin-loaded solid lipid nanoparticles for epidermal targeting, *J Control Release,*110: 296-06.
6. Cortesi R., Esposito E., Luca G., Nastruzzi C., (2000), Production of lipospheres as carriers for bioactive compounds, *Biomaterials*, 23:2283-94.
7. Domb A.J., (1993), United States Patent, USS 188837.
8. Ferrari M (2005) Cancer nanotechnology: opportunities and challenges. *Nat Rev Cancer* 5, 161– 171.
9. Fry D. W., White J. C., Goldman, I. D., (1978), Rapid separation of low molecular weight solutes from liposomes without dilution, *J Anal Biochem,* 90: 809-15.
10. Gajbhiye V, Kumar PV, Tekade RK, Jain NK (2007) Pharmaceutical and biomedical potential of PEGylated dendrimers. *Curr Pharma Design* 13, 415-429.
11. Gajbhiye V, Kumar PV, Tekade RK, Jain NK (2009) PEGylated PPI dendritic architectures for sustained delivery of H2 receptor antagonist. *E J Med Chem* 44, 1155-1166.
12. Gasco M.R., (1993), Method for producing solid lipid microspheres having narrow size distribution, United State Patent, US 188837.
13. Gasco M.R., (1997), Solid lipid nanospheres from warm microemulsions, *Pharm. Tech. Eur*., 9:52-8.

14. Gosselin P.M., Thibert R., Preda M., McMullen J.N., (2003), Polymeric properties of micronized carbamazepine produced by RESS, *Int J Pharm*, 252:225-33.
15. Hayes M.E., Drummond D.C., Kirpotin D.B.,(2006), Selfassembling nucleic acid-lipid nanoparticles suitable for targeted gene delivery, *Gene Ther*,13:646-51.
16. Heimbach JK, Kulik LM, Finn RS, Sirlin CB, Abecassis MM, Roberts LR, Zhu AX, Murad MH, Marrero JA. AASLD guidelines for the treatment of hepatocellular carcinoma. Hepatology 2018 ;67(1):358-80.
17. Hu F. Q., Zhang Y., Du Y. Z., Yuan, H. (2008), Nimodipine loaded lipid nanospheres prepared by solvent diffusion method in a drug saturated aqueous system, *Int J Pharm* 348:146– 52.
18. Indian Pharmacopoeia (1996,2011). Govt of India, Ministry of Health and Family Welfare. New Delhi, 1, 323
19. Jain NK (2001) Advances in Controlled and Novel Drug Delivery. *CBS Publishers and Distributors*, New Delhi, 1st ed. 40-69.
20. Jain RK, Stylianopoulos T (2010) Delivering nanomedicine to solid tumors. *Nat Rev Clin Oncol* 7, 653– 664.
21. Jenning V., Gysler A., Schafer K. M., Gohla S.,(2000), Vitamin A loaded solid lipid nanoparticles for topical use: Occlusive properties and drug targeting to the upper skin, *Eur J Pharm Biopharm*, 49:211-18.
22. Jenning V., Schafer-Korting M., Gohla S., (2000), Vitamin A-loaded solid lipid nanoparticles for topical use: drug release properties, *J Control Rel*, 66:115-26.
23. Jesse B, Mark W (2008). Therapeutic and diagnostic applications of dendrimers for cancer treatment. *Adv Drug Deliv Rev* 52, 1037-1065.
24. Kateb B, Chiu K, Black KL, Yamamoto V, Khalsa B, Ljubimova JY, Ding H, Patil R, Portilla-Arias JA, Modo M, Moore DF, Farahani K, Okun MS, Prakash N,Neman J, Ahdoot D, Grundfest W, Nikzad S, Heiss JD (2011) Nanoplatforms for constructing new approaches to cancer treatment, imaging, and drug delivery: what should be the policy? *Neuroimage* 1, S106-124.
25. Kojima C, Kono K, Maruyama K, Takagishi T (2000) Synthesis of PAMAM dendrimers having PEG grafts and their ability to encapsulate anti-cancer drugs. *Bioconj Chem* 11, 910-917.
26. Kumar SS, Saha AK, Kavitha K, Basu SK. Evaluation of clobazam loaded ionically cross-linked microspheres using chitosan. Der Pharmacia Sinica. 2012;3(6):616-23
27. Lan M, Zhu L, Wang Y. Multifunctional nanobubbles carrying indocyanine green and paclitaxel for molecular imaging and the treatment of prostate cancer. *J* Nanobiotechnology 2020; 18: 121-125.
28. Leamon CP, Low PS (1994) Selective targeting of malignant cells with cytotoxin-folate conjugates. *J Drug Target* 2,101-112.
29. Lee RJ, Low PS (1994) Delivery of liposomes into cultured KB cells via folate receptor-mediated endocytosis. *J Biol Chem* 269, 3198– 3204.
30. Lee RJ, Wang S, Low PS (1996) Measurement of endosome pH following folate receptor-mediated endocytosis. *Biochim Biophys Acta.*1312, 237-242.
31. Ler R., Manger W., Scouloudis M., Ku A., Davis C., Lee A., (2000), Solid Lipid Nanoparticles : A review *Biotech. Progress*, 16: 80-85.

32. Li S, Wei J, Yuan L, et al. RGD-modified endostatin peptide 530 derived from endostatin suppresses invasion and migration of HepG2 cells through the αvβ3 pathway. CancerBiotherRadio-pharmaceutics 2011; 26: 529–538.
33. Liang HF, Chen CT, Chen SC, Kulkarni AR, Chiu YL, Chen MC, Sung HW. Paclitaxel-loaded poly (γ-glutamic acid)-poly (lactide) nanoparticles as a targeted drug delivery system for the treatment of liver cancer. Biomaterials 2006;27(9):2051-2059.
34. Liang HF, Chen CT, Chen SC, Kulkarni AR, Chiu YL, Chen MC, Sung HW. Paclitaxel-loaded poly (γ-glutamic acid)-poly (lactide) nanoparticles as a targeted drug delivery system for the treatment of liver cancer. Biomaterials 2006;27(9):2051-9.
35. Liu X, Wang W, Wang Z. Recent progress in understanding the effects of autophagy in hepatocellular carcinoma. Chinese Journal of Hepatobiliary Surgery2014; 20: 69–73.
36. Llovet JM, Ricci S, Mazzaferro V, Hilgard P, Gane E, Blanc JF, De Oliveira AC, Santoro A, Raoul JL, Forner A, Schwartz M. Sorafenib in advanced hepatocellular carcinoma. New England journal of medicine 2008 ;359(4):378-90.
37. Lu B., Xiong S.B., Yang H., Yin X.D., Chao R.B.,(2006), Solid lipid nanoparticles of mitoxantrone for local injection against breast cancer and its lymphnode metastases, *Eur J Pharm Sci*, 28:86-95.
38. Ma KW, Cheung TT. Surgical resection of localized hepatocellular carcinoma: patient selection and special consideration. Journal of hepatocellular carcinoma 2017;4:1